INORGANIC
CHEMISTRY
FRONTIERS

Accepted Manuscript

Rational construction of metal-organic frameworks for heterogeneous catalysis

Sha Ou and Chuan-De Wu*

Center for Chemistry of High Performance and Novel Materials, Department of Chemistry, Zhejiang University, Hangzhou, 310027, P. R. China

E-mail: cdwu@zju.edu.cn

Abstract:

Metal-organic frameworks (MOFs) are a class of porous materials, which consist of highly ordered organic building blocks and metal ions/clusters. Because the emerging porous materials have the ability to retain and even enhance the individual functionalities of the secondary building units (SBUs), the catalytic functions of porous MOFs can be therefore easily realized by carefully choosing and tuning the functional moieties in building synthons. Accompanying the development on the synthesis strategy and the characterization technology for MOF materials, the MOF catalysts have been undergone upsurge, which have been transcended the stage of opportunism. This brief review will give a cross-section on rational design and synthesis of porous metal-organic framework materials for heterogeneous catalysis.

1. Introduction

Metal-organic frameworks (MOFs) are an emerging class of crystalline porous materials, which are built from organic linkers connecting with metal ions/clusters through metal-ligand bondings.[1] Because of their fascinating topological structures and remarkable properties, the MOF materials have provided multiple entries into technologically useful materials for applications in the fields of gas storage, separation, magnetics, biomedicine, fluorescence, molecular recognition and heterogeneous catalysis.[2-9]

In principle, crystal engineering of porous MOFs can be regarded as self-assembly and self-organization of connectors of metal ions/clusters and linkers of organic building synthons under mild reaction conditions. The topological structures of MOFs are majorly defined by the coordination geometries of metal nodes and the directionalities of organic ligands. The major objective of current crystal engineering of MOF materials is to vary the metal connectors and the organic linkers for the construction of desired porous functional materials for target applications. Even though many synthesis strategies and characterization technologies for the MOF materials have been explosively developed, however, there are still many difficulties to precisely predict and control the overall topological structures from their chemical compositions, because combination of the metal nodes and organic linkers are affected by many factors, such as solvent, temperature, reaction duration, concentration, counter ion and pH-value. Nevertheless, it is feasible to rationally introduce catalytic-active moieties into porous MOFs by carefully modifying the organic/inorganic moieties, and thus realize their heterogeneous catalytic properties.

Considering that many reviews have been comprehensively discussed on the catalytic applications of MOFs, this short review only gives a cross-section on rational design and synthesis of the functional moiety oriented MOFs for heterogeneous catalysis.[9] The selectively grafted functional moieties on the pore surfaces of MOFs let them exhibit interesting catalytic properties with remarkable size- and shape-selectivities, which cannot be matched by the traditional inorganic zeolites.[10]

2. The principle for design of metal-organic framework catalysts

Generally speaking, most MOFs have a certain degree of catalytic activities on the reactions that are dependent on the sites of metal/cluster nodes and/or the organic moieties. Even though the metal sites are fully ligated by strongly coordinated organic ligands, there are still abundant unsaturated metal coordination sites on the surfaces of MOFs because of the coordination defect. If the metal coordination sites are partially terminated by volatile solvent molecules, such as water, alcohols, acetonitrile and DMF, *etc.*, these MOF materials will be efficient on some catalytic reactions that are prompted by the metal nodes. This is because these MOFs are easily activated to generate unsaturated metal coordination sites by removal of the volatile solvent molecules under suitable conditions. However, because these metal ions are also the pivot components of MOFs, the framework structures are easy collapse during catalysis. For example, the well known porous MOF HKUST-1 is built from paddle-wheel $Cu_2(COO)_4$ secondary building units (SBUs) linked by benzene 1,3,5-tricarboxylate.[11] The axial coordination sites of Cu^{II} ions are occupied by weakly bound water molecules, which can be removed by simply heating the compound in vacuum. Dehydration makes the copper Lewis acid centers highly catalytic-active, which can coordinate with organic substrates to result in an activation of the catalytic process, such as cyanosilylation of benzaldehyde.[12] However, because the Cu^{II} ions are easily reduced by aldehyde molecules under the catalytic reaction conditions, HKUST-1 is partially decomposed during catalysis.

Obviously, using the above method on the synthesis of MOF catalysts is not a good choice. Therefore, several effective strategies have been well developed, which have been gradually maturing. The most straight forward strategy is to use catalytic-active moieties as building synthons to synthesize organic linkers. Those catalytic-active ligands can well define the catalytic properties of the resulting porous metal-organic materials. To date, numerous catalytic-active moieties have been successfully immobilized onto the pore surfaces of porous MOFs, which present remarkable catalytic activities with interesting size- and shape-selectivities.[12] The catalytic-active moieties include metallosalens, metalloporphyrins, amino acids,

3

carbenes and polyoxometalates, *etc*. Because there are still many difficulties on the construction of highly porous MOFs in practical procedures, it is impossible to introduce any homogeneous catalytic-active moieties into the crystalline porous materials in "one-pot" synthesis. Therefore, post-synthetic modification is developed as an alternative strategy for the construction of metal-organic framework catalysts.[13] Those porous metal-organic materials, consisting of post-modifiable moieties on the building blocks, can be easily functionalized with suitable functional moieties to generate highly efficient porous MOF catalysts.

3. Coordinatively unsaturated metal nodes as catalytic-active sites

There have been a large number of MOFs whose coordination sites of metal nodes are unsaturated or occupied by volatile solvent molecules, such as water, alcohols, acetonitrile and DMF, *etc*. The formers can be directly used for catalysis without requirement of special activation, whereas the later ones should be carefully activated to remove the volatile solvent ligands on metal nodes to generate coordinatively unsaturated metal sites for heterogeneous catalysis.

The supramolecular solid, $[Cu_2L^1_2(DMF)_2(H_2O)_2]$ (**1**), built from 1,8-naphthalenecarboxylic anhydride-4,5-dicarboxylicate (L^1) linking up binuclear copper(II) synthons, is very stable in common organic solvents because the binuclear copper(II) units are strongly connected via multiple supramolecular contacts (Fig. 1).[14] The copper(II) ion in the supramolecular solid is in a distorted square-planar coordination geometry, which can directly provide the vacant axial positions to coordinate with substrate molecules during heterogeneous catalysis. Prompted by the supramolecular solid **1**, the arylboronic acid and imidazole substrates were smoothly transferred to the desired cross-coupling products (up to 96.8% yield) under mild conditions. Moreover, the solid catalyst **1** can be simply recovered by filtration, which was reused for six consecutive cycles without significantly deterring the catalytic efficiency.
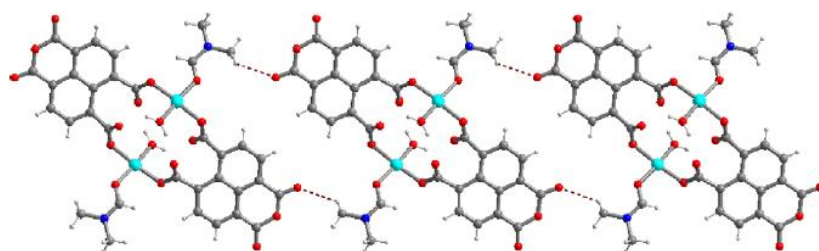
**Fig. 1** Supramolecular solid **1** built from $[Cu_2L^1{}_2(DMF)_2(H_2O)_2]$ units (Cu, cyan).

The 1D coordination polymer $[Cu(L^2)_2]$ (**2**) is built from an amino acid derivative L^2 (HL^2 = N-(4-pyridyl)-D,L-Valine) bridging Cu^{II} ions.[15] In the crystal structure of **2**, the copper ion coordinates to two carboxyl oxygen atoms and two pyridyl groups of four L^2 ligands in a square-planar coordination geometry. Two L^2 ligands *trans*-link two Cu^{II} centers to form an 18-membered macrocycle ring, which is further propagating into a 1D polymeric chain (Fig. 2). Since the square-plane coordinated Cu^{II} ion has two vacant axial positions, compound **2** efficiently prompted the catalytic cross-coupling reaction of arylboronic acids with imidazole at room temperature, which generated the anticipated products of *N*-phenylimidazoles in good yields (up to 97%). The catalytic activity of **2** is highly dependent on the solvent media. When different solvents, such as DMF, THF, CH_2Cl_2 and H_2O, were used instead of MeOH, almost no product can be produced except for trace product from the solvent of DMF, which suggests that there is a competed coordination to Cu ions between the solvent and substrate molecules.
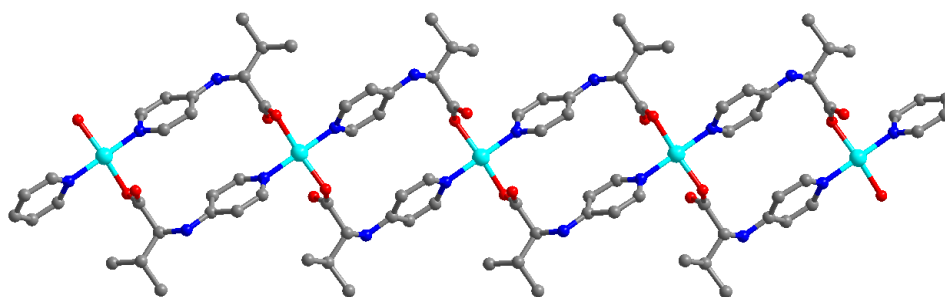
Fig. 2 The 1D polymeric chain network of compound **2** (Cu, cyan).

With the help of mixed ligands in multiple coordination modes, different

coordination geometries of the metal nodes can be simultaneously generated in a porous MOF, which often consists of the active metal sites that are either coordinatively vacant or coordinated to volatile solvent molecules. In the structure of $[Cu_3(pdtc)L^3_2(H_2O)_3]$·guest (**3**; H_4pdtc = pyridine-2,3,5,6-tetracarboxylic acid; HL^3 = (E)-4-(2-(pyridin-4-yl)vinyl)benzoic acid), two kinds of pyridine carboxylate ligands connect with copper nodes to form an interesting 3D porous framework.[16] As shown in Fig. 3, one third copper ions, which are exposed on the interior surface of the 1D channel walls (13.76 $\times$ 23.62 $Å^2$), coordinate to volatile water molecules that are readily substituted by suitable molecules. Single crystal structural analysis demonstrates that the water ligands can be replaced by pyridine and EtOH molecules, whereas the overall framework is almost intact. The immobilized catalytic-active copper(II) centers in the channel walls can trigger the Henry reaction of benzaldehydes with nitroalkanes, in which up to 85% product yield has been achieved. The catalytic property of **3** is much superior to that of simple copper salts because the homogeneous metal coordination sites are easily ligated by the counter ions.
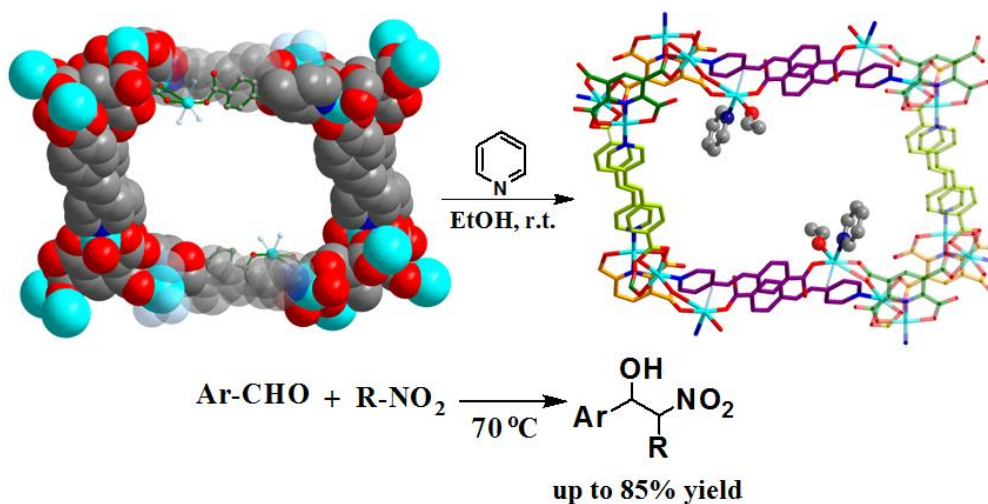
Fig. 3 The structural transformation of **3** in pyridine/EtOH solution, and the catalytic Henry reaction of benzaldehydes with nitroalkanes.

The catalytic properties of MOFs are very sensitive to the pore structures, even though their pore structures are slightly tuned, because the substrate and product molecules are transported through the opening channels. The neutral 2D MOF

$[Mn_2L^4{}_2(H_2O)_2]$ $3H_2O$ (**4**; H_2L^4 = E-5-(2-(pyridin-4-yl)vinyl)isophthalic acid) is built from octahedrally coordinated Mn^{II} ions linked by L^4 ligands with cavity dimensions of 7.80 × 8.94 $Å^2$ (Fig. 4).[17] In the crystal structure of **4**, the Mn^{II} center is oriented towards the 1D channels, and coordinates to one labile water molecule. Therefore, the Mn centers are active on the oxidation of phenylmethanol, which produces the oxidation product benzaldehyde in 64% yield when the reaction was performed at 60 °C for 18 h. Interesting is that two neighboring C=C centers in two layers are at a reasonable distance, which let compound **4** undergo topochemical [2+2] cycloaddition in a single-crystal-to-single-crystal (SCSC) manner from a 2D to a 3D structure transformation under a UV light radiation. Compared with the structure of **4**, two C=C centers from two original neighboring layers form a cyclobutane ring in the porous network of $[Mn_2L^5(H_2O)_2]$ $3H_2O$ (**5**; H_4L^5 = 5,5'-(3,4-diphenylcyclobutane-1,2-diyl)diisophthalic acid). Even though the pore volume is slightly increased (from 24.3% to 27.0%), however, the catalytic activity of **5** is significantly improved, which generates the oxidation product benzaldehyde in 97% yield under otherwise identical conditions. The above results demonstrate that the pore structures of MOF catalysts play a very important role on the catalytic performance of active sites inside the pores.
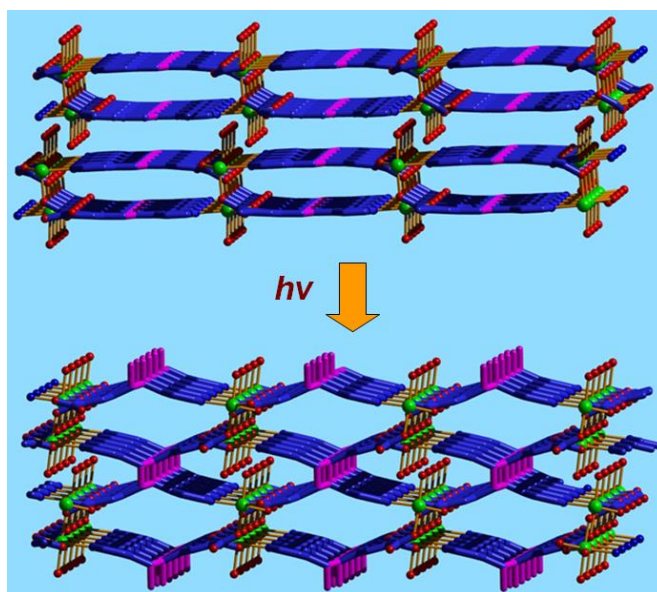

Fig. 4 The UV irradiated SCSC structural transformation from 2D layered network of **4** (above) to 3D porous framework of **5** (below).

## 4. Metal-organic framework catalysts constructed from metallosalens

Salens, the condensation products of aryl aldehydes and diamines, are a class of universal and excellent ligands to chelate various metal ions for the synthesis of different metallosalen catalysts.[18] Metallosalens have been realized different catalytic properties with remarkable enantio-selectivities in a variety of reactions. Therefore, metallosalens are the excellent synthons for the synthesis of porous MOF catalysts, which have been realized heterogeneous catalytic applications on alkene epoxidation, cyclopropanation and hydrolytic kinetic resolution of epoxides with interesting size-, shape- and enantio-selectivities.

A chiral bipyridyl Mn-salen ((R,R)-(2)-1,2-cyclohexanediamino-*N,N'*-bis(3-tert-butyl-5-(4-pyridyl)salicylidene)$Mn^{III}Cl$ = L^6) together with a biphenyldicarboxylate (bpdc) was used to connect with paddle-wheel $Zn_2(COO)_4$ SBUs for the construction of a homochiral porous MOF $[Zn_2(bpdc)_2L^6]$ guest (**6**), which is highly efficient on asymmetric epoxidation of olefins (Fig. 5).[19] The catalytic-active Mn^{III} species, incorporated in the Mn-salen units, are accessible to substrate molecules transported through the opening channels (6.2 $\times$ 15.7 $Å^2$ in dimensions). The heterogeneous catalytic oxidation of 2,2-dimethyl-2H-chorome by 2-(tertbutylsulfonyl)iodosylbenzene gives the epoxide product with an *ee* value of 82%. To prove that the catalysis occurs inside the pores of **6**, a mixture of large porphyrin substrate (larger than the channel sizes of **6**) and a small ethyl 4-vinyl benzoate substrate (smaller than the channel sizes of **6**) in 1 : 1 olefinic unit ratio was reacted with 2-(tertbutylsulfonyl) iodosylbenzene in the presence of heterogeneous **6** or homogeneous Mn-salen. The different catalytic properties of **6** and homogeneous Mn-salen on oxidation of the mixed substrates have proved that the heterogeneous catalysis chiefly occurs inside the pores of solid catalyst **6**.
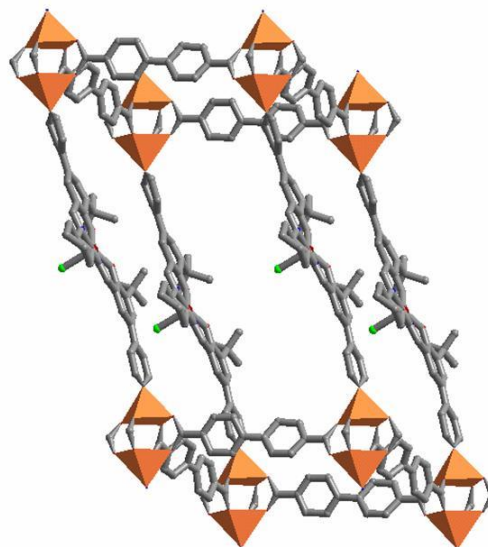
Fig.5 The 3D porous structure of **6** constructed from Mn-salen and paddle-wheel $Zn_2(COO)_4$ SBUs.

As shown in Fig. 6, the Lin group has synthesized a family of isoreticular chiral metal-organic frameworks (CMOFs) $[Zn_4(\mu_4\text{-O})(Mn\text{-salen})_3]$ guest (CMOFs 1-5), which are built from $[Zn_4(\mu_4\text{-O})(O_2CR)_6]$ SBUs and chiral Mn-Salen catalytic centers ((R,R)-1,2-cyclohexanediamino-N,N'-bis(3-tert-butyl-salicylidene)$Mn^{III}Cl$) with systematically elongated dicarboxylate bridges (–COOH, –CH=CHCOOH, and –C_6H_4COOH groups terminated on the 4,4'-positions of Mn-Salen).[20] The pore structures and the pore sizes of these CMOFs are systematically dependent on the spacers of the tunable dicarboxylate bridges and the steric sizes of the solvents with the open channel dimensions varied from 8×6 Å^2 to 25×23 Å^2. CMOFs 1-5 are highly efficient on catalyzing asymmetric epoxidation of a number of olefins, whereas the epoxidation rates were shown to be strongly dependent on the open channel sizes of CMOFs, in which up to 92% *ee* has been achieved for the asymmetric epoxidation of chromene to generate (1R,2S)-indene oxide. These results demonstrate that larger open channels can facilitate diffusion of the reactant and product molecules to increase the catalytic reaction rates.
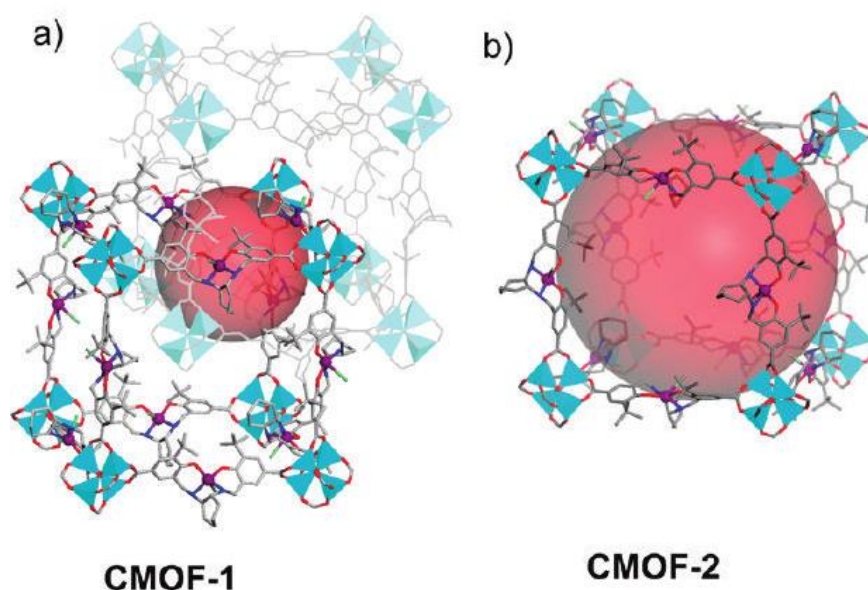
Fig. 6 The structures of the interpenetrated network of CMOF-1 and the non-interpenetrated network of CMOF-2.

They also studied the catalytic properties of a pair of CMOFs $\{Zn_4(\mu_4\text{-O})\text{-}[(Ru^{III}\text{-salen})(py)_2Cl]_3\}$ guest (CMOFs 7 and 8), based on Ru-salen-dicarboxylate.[21] The largest cavities in the interpenetrated network of CMOF-7 are of 8 Å in diameter with the corresponding pore windows of 4×3 Å^2 in dimensions, whereas those of the non-interpenetrated framework of CMOF-8 are of 17 Å and 14×10 Å^2, respectively. The Ru^{III} centers in the as-synthesized CMOFs 7 and 8 can be reduced to Ru^{II} centers by strong reducing agents such as LiBEt$_3$H or NaB(OMe)$_3$H in a reversible SCSC manner. The resulting non-interpenetrated Ru^{II}-CMOF was highly active on the asymmetric cyclopropanation of substituted alkenes with very high diastereo- and enantio-selectivities (*d.r.* = 7 : 1 (trans/cis); *ee* = 91% (trans) and 84% (cis)). In contrast, the interpenetrated Ru^{II}-CMOF was nearly inactive (less than 1% yield), probably because the small channels cannot transport the substrate molecules, thus preventing the diffusion of the reagents to access the Ru^{II}-salen active sites in the interior pore surfaces.

The Cui group has reported a homochiral MOF, [Cd$_4$(Co^{III}-salen)$_4$(DMF)$_4$(OAc)$_4$] 4H$_2$O (**7**), based on a Co-salen-dicarboxylate (Fig.

7).[22] The 3D chiral porous framework of **7** is built from square-planar tetrameric [Cd$_4$(O$_2$C)$_8$] SBUs connected with Co-salen linkers with open channel dimensions of 12 × 8 Å^2 along the *a* axis. The catalytic-active Co-salen sites are accessible to substrate molecules via the open channels, which can efficiently prompt the heterogeneous asymmetric hydrolytic kinetic resolution of a range of benzyloxy epoxide derivatives with *ee* value up to 99.5%. Since the heterogeneous catalysis mainly occurs inside the pores of the Co-salen MOF, it has size-selective property. The conversion for the small substrate phenoxy epoxide is of 56%, whereas the conversion for the sterically bulky substrate triphenyl glycidyl ether is less than 5% under the same reaction conditions because the bulky substrate has difficult to access the catalytic sites inside the pores.
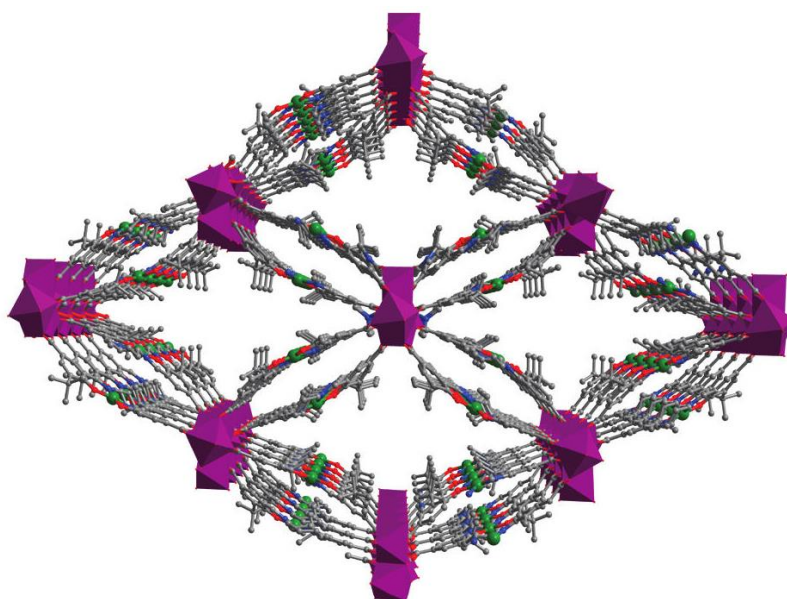

Fig. 7 The 3D porous structure of **7** (Cd, purple polyhedra).

5. Metal-organic framework catalysts constructed from metalloporphyrins

Metalloporphyrins are the active sites in monooxygenases which can efficiently oxidize a variety of organic molecules under mild conditions.[23] The rigid macrocycle rings make metalloporphyrin moieties be an ideal class of building blocks for the construction of highly porous MOFs. Incorporation of metalloporphyrin moieties into the emerging porous MOF materials not only can retain and even enhance the

functionalities of the building blocks, but can also improve the stability of metalloporphyrins in oxidation catalysis.[24] Furthermore, the different catalytic functionalities of the porous porphyrinic framework materials can be easily targeted by modulating the porphyrin metal sites and tailoring the peripheral environments of metalloporphyrins. Among the reported porphyrinic MOFs, the bridging moieties and the configurations of metalloporphyrins have played crucial roles on tuning and stabilizing the pore structures of porphyrinic MOFs.

The porphyrinic MOF $[Zn_2(HCOO)(Fe^{III}(H_2O)\text{-}TCPP)]$ (**8**) is a 3D porous structure that is built from formate pillars to connect with layered networks of Fe^{III}-TCPP moieties linking up paddle-wheel $Zn_2(COO)_4$ SBUs (Fig. 8).[25] In the crystal structure of **8**, the square-pyramidally coordinated iron(III) ions are accessible to the included solvent molecules in the pores. The solid catalyst is highly active on the aldol reaction of aldehydes and ketones. The yields of aldol products are excellent (up to 99%), which are superior to those of its homogeneous constituents, such as $FeCl\text{-}Me_4TCPP$, $Zn(NO_3)_2$ and $FeCl_3$.
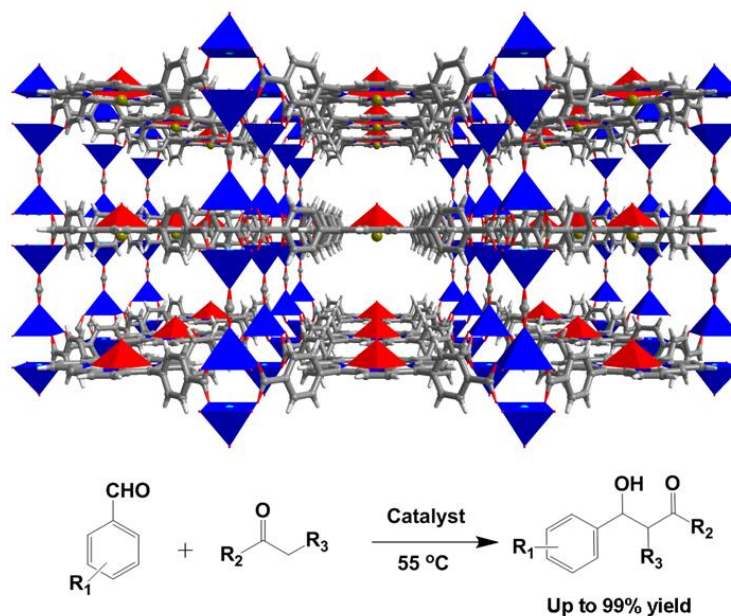
Fig. 8 Crystal structure of **8**, and the catalytic aldol reaction of aldehydes with ketones.

In some cases, the axial coordination sites of the porphyrin metal ions are ligated

by coordination donors in porphyrinic MOFs, which will obstruct their catalytic efficiency. As shown in Fig. 9, the active Mn^{III} sites in two isomorphous porphyrinic frameworks $[(CH_3)_2NH_2][Zn_2(HCOO)_2(Mn^{III}$-TCPP)] guest (**9**) and $[(CH_3)_2NH_2][Cd_2(HCOO)_2(Mn^{III}$-TCPP)] guest (**10**) are blocked by formate ligands, which make the active sites inaccessible to substrate molecules through the opening channels.[25] Even though they are highly active on the epoxidization of a number of olefins with different sizes and dimensions; however, because the catalytic-active sites are only available on the exterior solid surfaces with coordinative defect, the catalysis thus occurs on the solid surfaces of the porphyrinic MOFs, which present significant particle-size-effect on the oxidation rates.
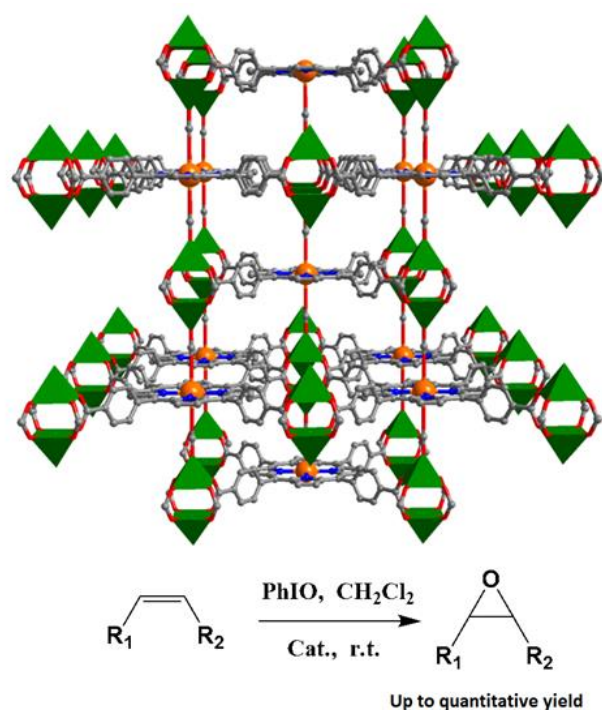
Fig. 9 A perspective view of the 3D porphyrinic framework **9** (Mn, orange), and epoxidation of olefins catalyzed by solid **9**.

Because the preferred coordination geometry of palladium(II) ions is square-plane, the axial coordination sites of porphyrin palladium(II) ions therefore are not ligated by coordination donors, as demonstrates in the porous coordination network $[Cd_{1.25}(Pd$-$H_{1.5}TCPP)(H_2O)]$ guest (**11**), in which the square-coordinated palladium(II) sites are exposed on the channel walls along with the tailored zeolitic

periphery (Fig. 10).[26] The styrene substrate can be fully oxidized into a mixture of 91% acetophenone and 9% benzaldehyde with H_2O_2 oxidant under mild conditions. The catalytic property of **11** is superior to that of its components of Pd-H_4TCPP, $PdCl_2$, Pd(OAc)$_2$ and Pd/C in the cases of the substrate conversions and the product selectivities. The single crystal structure and ^{1}H NMR spectroscopy clearly indicate that the styrene molecules are readily incorporated into the pores of **11**, which thus demonstrate that the catalytic reaction chiefly occurs inside the pores.
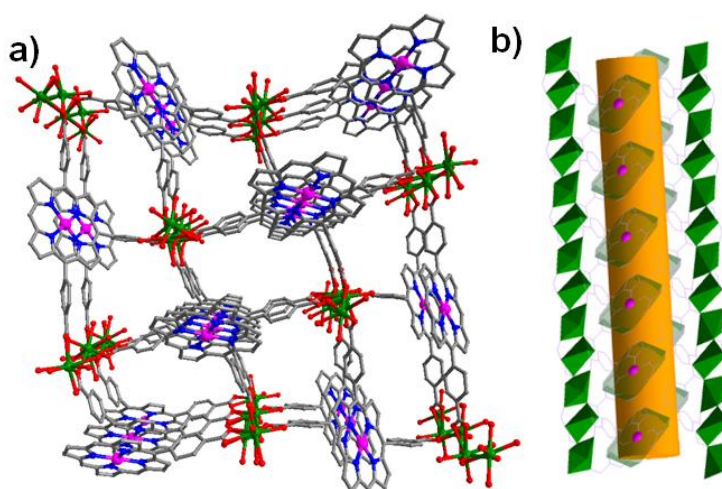
Fig. 10 (a) The 3D structure of **11** as viewed down the *a* axis, and (b) the 1D opening channel with accessible Pd^{II} sites in **11**.

The three isostructural porous porphyrinic MOFs, [Mn$_5$Cl$_2$(MnCl-OCPP)(DMF)$_4$(H$_2$O)$_4$] guest (ZJU-18), [Mn$_5$Cl$_2$(Ni-OCPP)(H$_2$O)$_8$] guest (ZJU-19) and [Cd$_5$Cl$_2$(MnCl-OCPP)(H$_2$O)$_6$] guest (ZJU-20) demonstrate that metal-5,10,15,20-tetrakis(3,5-biscarboxylphenyl)porphyrin (M-H$_8$OCPP), containing four *m*-benzenedicarboxylate moieties, is powerful on construction and stabilization of highly porous coordination frameworks.[27] In the crystal structure of ZJU-18, Mn^{III}Cl-OCPP is linked by two kinds of binuclear Mn$^{II}_2$(COO)$_4$Cl$_2$ and trinuclear Mn$^{II}_3$(COO)$_4$(μ-H$_2$O)$_2$(H$_2$O)$_6$ metal carboxylate SBUs to form a 3D porous structure of *tbo* net, which consists of large pore cages of about 21.3 Å and the pore windows are of about 11.5 Å in diameters (Fig. 11). ZJU-18 is highly efficient on selective oxidation of alkylbenzenes (>99% yield of acetophenone).

The high oxidation efficiency of ZJU-18 should be attributed the cooperative effect between the catalytic-active metal nodes and the porphyrin metal ions. This conclusion has been proved by the catalytic properties of ZJU-19 and ZJU-20, because the conversion of ethylbenzene is of 9% oxidized by ZJU-19 with active metal nodes only, and of 69% oxidized by ZJU-20 with active Mn^{III}-porphyrins only. The catalytic activity and stability of ZJU-18 are also much superior to those of the homogeneous $Mn^{III}Cl$-Me_8OCPP counterpart (>99% conversion for ZJU-18 *vs.* 16% for $Mn^{III}Cl$-Me_8OCPP, and sustained 15 cycles *vs.* deactivated at the third cycle).
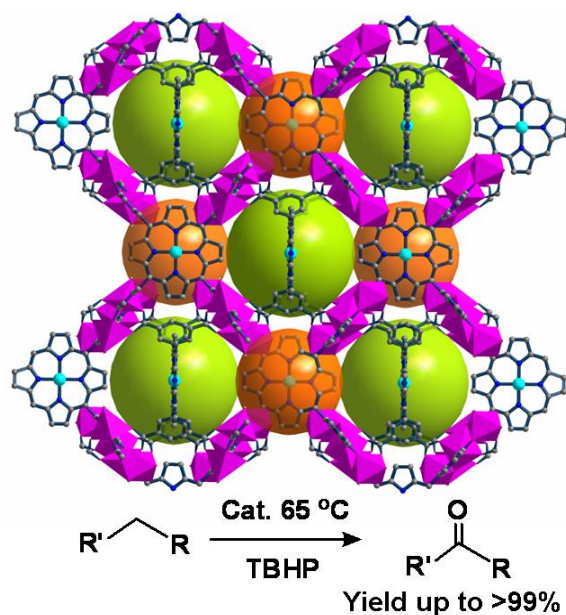

Fig. 11 Crystal structure of ZJU-18 built from $Mn^{III}Cl$-OCPP linking up binuclear and trinuclear Mn-carboxylate SBUs, and catalytic oxidation of alkylbenzenes by ZJU-18.

The two robust porphyrinic frameworks [$Cu_4(Ni$-$OCPP)(H_2O)_4$] guest (ZJU-21) and [$Cu_{16}(Mn^{III}OCPP)_3(OH)_{11}(H_2O)_{17}$] guest (ZJU-22) are very stable in various different solvents, even in acidified aqueous solution.[28] As shown in Fig. 12, ZJU-21 is built from paddle-wheel $Cu_2(COO)_4$ SBUs and octatopic metalloligand Ni-OCPP, forming nanopore cages (2.1 nm in diameter). The structure of ZJU-22, containing 1D nanotubular channels of 1.5 nm in diameter, is a unique 3D framework constructed from three independent nets which are interconnected and stabilized by the Mn-OH-Cu bridges. ZJU-21 and ZJU-22 exhibit pore structure dependent catalytic activities in the cross-dehydrogenative coupling (CDC) reaction of tertiary

15

amines and nitroalkanes under solvent free conditions (up to 97% yield) or in water (up to 93% yield) at room temperature.
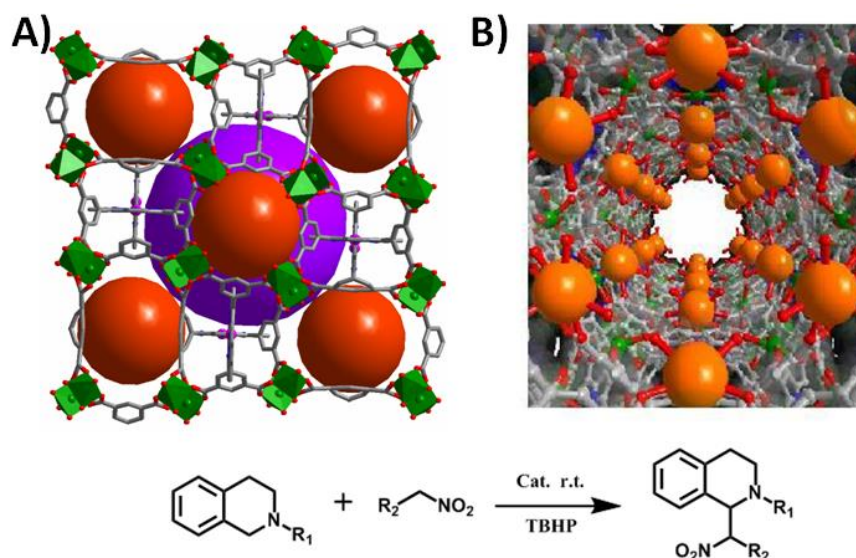
Fig. 12 Crystal structures of the 3D porous ZJU-21 (A) and ZJU-22 (B), and the catalytic CDC reaction of 1,2,3,4-tetrahydroisoquinoline derivatives and nitroalkanes.
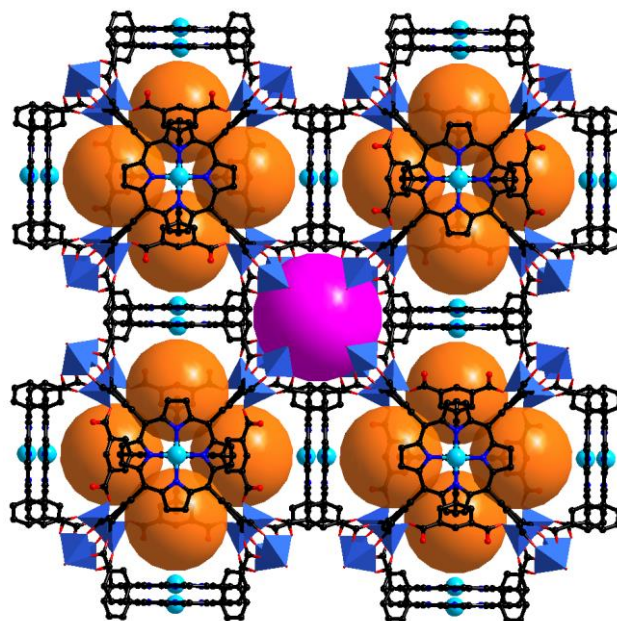
Fig. 13 Crystal structure of CZJ-4, containing two kinds of cages and substrate accessible Mn^{III} sites inside the cages.

To make use of Mn^{III}Cl-OCPP connecting with paddle-wheel $Zn_2(COO)_3$ SBUs, a porous porphyrinic framework material CZJ-4, whose structure consists of two kinds

of cages and open windows of about 1.0 nm in diameter, is successfully constructed (Fig. 13).[29] Immobilization of Mn^{III}-porphyrins onto the pore surfaces of MOF, CZJ-4 exhibits high catalytic efficiency, selectivity and stability on epoxidation of olefins, in which high conversions (up to 100%) and selectivities (up to 94% epoxide product) have been achieved in the oxidation of small olefins. The catalytic property of heterogeneous CZJ-4 is superior to that of the homogeneous $Mn^{III}Cl\text{-}Me_8OCPP$ in terms of substrate conversion and product selectivity. Because the large substrates have difficulty to access the interior pores, CZJ-4 demonstrates excellent substrate size-selectivity in the heterogeneous epoxidation catalysis.
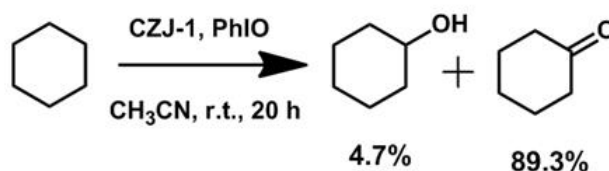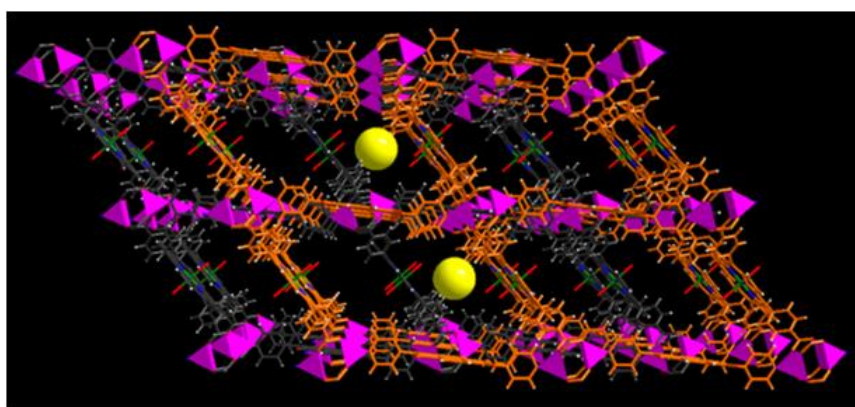

Fig. 14 Crystal structure of CZJ-1 with uniformly immobilized Mn^{III} sites on the pore surfaces, and highly efficient oxidation of cyclohexane catalyzed by CZJ-1.

The porphyrinic framework $[Zn_2(Mn^{III}OH\text{-}TCPP)(DPNI)]$ guest (CZJ-1; DPNI = N,N′-di-(4-pyridyl)-1,4,5,8-naphthalenetetracarboxydiimide) is a doubly interpenetrated structure (Fig. 14).[30] In the structure of CZJ-1, the paddle-wheel $Zn_2(COO)_4$ SBUs are bridged by $Mn^{III}OH\text{-}TCPP$ to form 2D sheets which are further connected by DPNI to form the 3D porous structure with substrate accessible pore channels of about 6.1×7.8 Å^2 in dimensions. CZJ-1 exhibits high catalytic activity on the epoxidation of styrene at room temperature, in which styrene can be almost fully

oxidized into the epoxide product (97% selectivity), and the turnover number is up to 14068. Remarkably, the most inert cyclohexane substrate can be almost quantitatively oxidized by CZJ-1 at room temperature (94% conversion). The high efficiency of CZJ-1 on activation of the inert substrate should be attributed to the collaborative work effects of multiple species, including the secondary catalytic-active DPNI moieties, in the pores. The fundamental basis, to prove that the catalysis mainly takes place inside the pores and the inside active sites are accessible to the included substrate molecules, is evident from the single crystal structures of CZJ-1$\supset$2styrene and CZJ-1-Ti that are transferred from CZJ-1 in SCSC transformations.

The porphyrin-POM hybrid framework, $\{[Cd(MnTPyP)](PW_{12}O_{40})\}$, is built from Cd-Mn-TPyP layers and interlayer inserted $[PW_{12}O_{40}]^{3-}$ anions (Fig. 15). The hybrid material can efficiently oxidize alkylbenzene with tertbutylhydroperoxide (TBHP) oxidant.[31] $\{[Cd(MnTPyP)](PW_{12}O_{40})\}$ oxidizes ethylbenzene to form one product of acetophenone (92.7% yield), which is superior to those of its precursors, such as $Mn^{III}Cl$-TPyP (73.6% yield) and $[PW_{12}O_{40}]^{3-}$ (inactive). Because oxidation mainly occurs inside the pores, $\{[Cd(MnTPyP)](PW_{12}O_{40})\}$ presents excellent size selectivity in the oxidation of a series of alkylbenzene.
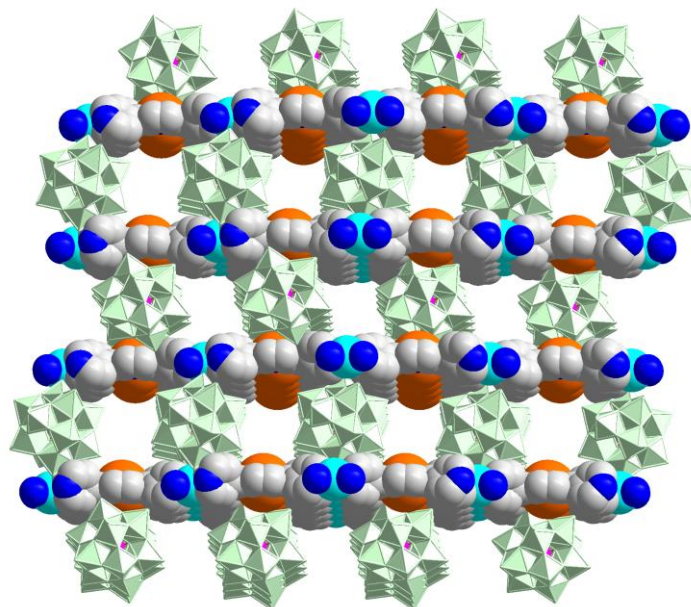
Fig. 15 The porous structure of $\{[Cd(MnTPyP)](PW_{12}O_{40})\}$, consisting of alternative layers of anionic POMs and cationic Mn^{III}-porphyrin nets (Mn^{III}, orange).

Metalloporphyrins are the excellent light sensitizers in photosynthesis. Immobilization of metalloporphyrins onto the pore surfaces of MOFs can achieve outstanding stability and photoactivity in heterogeneous phases. The 3D porous porphyrinic MOF, $[Zn_2(H_2O)_4Sn^{IV}(TPyP)(HCOO)_2]$ guest (**12**), is constructed from lamellar networks of photoactive tin(IV)-porphyrin ($Sn^{IV}TPyP$) building blocks linking up Zn^{II} ions, which are further connected by formates to coordinate with the Sn^{IV} centers (Fig. 16).[32] MOF **12** exhibits remarkable photocatalytic activities on photo-oxygenation of phenol and sulfides under visible light irradiation, resulting in almost quantitative conversions with remarkable selectivity (>99%) in heterogeneous phases. The catalytic property of the heterogeneous catalyst **12** is much superior to that of the homogeneous counterpart $Sn^{IV}(OH)_2TPyP$ under the identical conditions, in terms of the catalytic activity and stability.
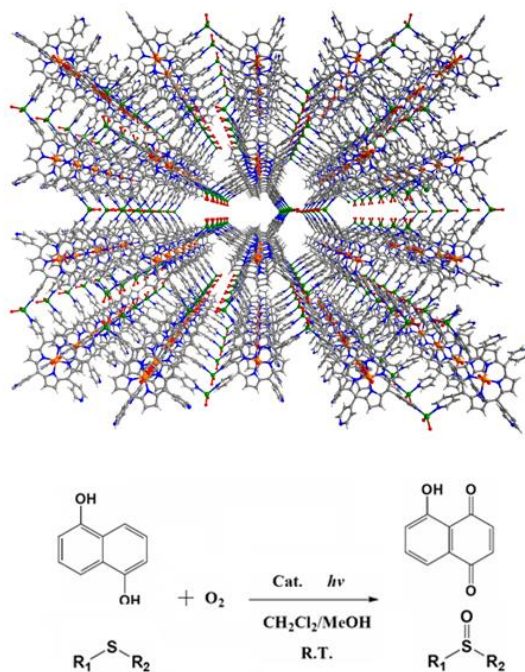
Fig. 16 The structure of **12** and its application in photo-oxidation of phenol and sulfides.

Encapsulating porphyrins and metalloporphyrins as guests or templates in the pores of MOFs in "one-pot" synthesis is an alternative strategy to stabilize the active metalloporphyrin sites in a "ship-in-a-bottle" configuration, which can prohibit

self-dimerization and oxidative degradation of the metalloporphyrins. Eddaoudi *et al*. have encapsulated 5,10,15,20-tetrakis(1-methyl-4-pyridinio)porphyrin (H$_2$TMPyP) into an indium imidazoledicarboxylate-based *rho*-ZMOF host to generate a unique and tunable catalyst platform of H$_2$RTMPyP (Fig. 17).[33] The catalytic property of the platform can be systematically tuned by metallation of the metal-free porphyrins with different metal ions of Mn, Cu, Zn and Co ions via post-synthesis. They proved that Mn-RTMPyP is active on oxidation of cyclohexane to cyclohexanol/cyclohexanone in 91.5% yield with turn over number of 23.5 (based on the consumed oxidant).
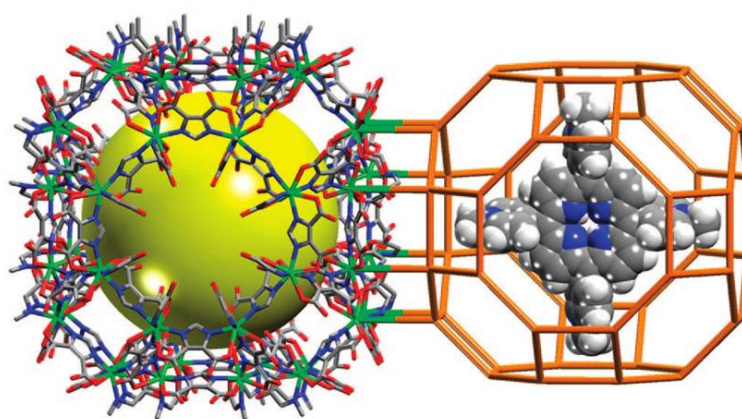

Fig. 17 Crystal structure of *rho*-ZMOF (left) and schematic presentation of [H$_2$TMPyP]$^{4+}$ porphyrin enclosed in *rho*-ZMOF cage (right).

6. Metal-organic framework catalysts constructed from amino acid moieties

Natural amino acids are the basic building units and the functional moieties in biological organisms, which have special biological activities and selective substrate-binding functions. Limited by their few available coordination donors and flexible backbones, most amino acids do not have the ability to create and stabilize highly porous MOFs. Therefore, several effective strategies have been developed to immobilize amino acid synthons onto porous MOFs.[34]

We have reacted amino acids with aldehydes and further reduced to synthesize a series of amino acid derivatives.[35] The pyridyl group on Py-Ser ligand links up copper-amino carboxylate SBUs into a 2D bilayer framework [Cu$_2$(Py-Ser)$_2$Cl$_2$]·H$_2$O (**13**), containing multiple chiral centers (Fig. 18).[36] Compound **13** is highly active on

catalyzing the Biginelli reaction of benzaldehyde, urea and ethyl acetoacetate with 90% yield of dihydropyrimidinone; however, it does not exhibit any enantioselectivity. It is interesting that **13** efficiently catalyzes the reaction of asymmetric 1,2-addition of Grignard reagent to α,β-unsaturated ketones/aldehyde, up to 93% conversion and 99% *ee* value have been achieved, which are superior to those of Py-Ser ligand with 84% conversion and 51% *ee* value.
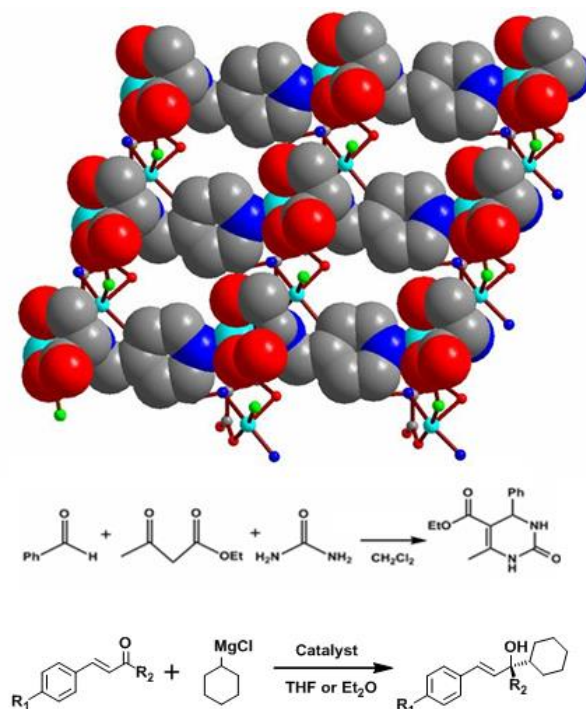
Fig. 18 Crystal structure of **13**, and Biginelli reaction of benzaldehyde, urea and ethyl acetoacetate, and 1,2-addition of α,β-unsaturated ketones catalyzed by compound **13**.

The Duan group has reported a homochiral 2D honeycomb coordination network Cd-BTB, which is building up from 1,3,5-tris(4-carboxyphenyl)benzene (H₃BTB) linking up cadmium(II) ions with rhombus channels of 4.0×6.5 Å^2 in dimensions (Fig. 19).[37] The chiral L-PYI (L-pyrrolidin-2-ylimidazole) moiety, derived from spontaneous deprotection of the Boc (*tert*-butoxycarbonyl) group on L-*N*-tertbutoxycarbonyl-2-(imidazole)-1-pyrrolidine (L-BCIP), is terminally coordinating to cadmium ions. It is interesting that L-PYI moieties are located above and below the 2D layer in Cd-BTB, which let Cd-BTB highly active on aldol reaction, in which 61% *ee* value has been achieved in the reaction between 3-nitrophenyl and

cyclohenanone. Because the small pore cannot accommodate substrate molecules, the catalytic reaction only occurs on the exterior solid surfaces of Cd-BTB.
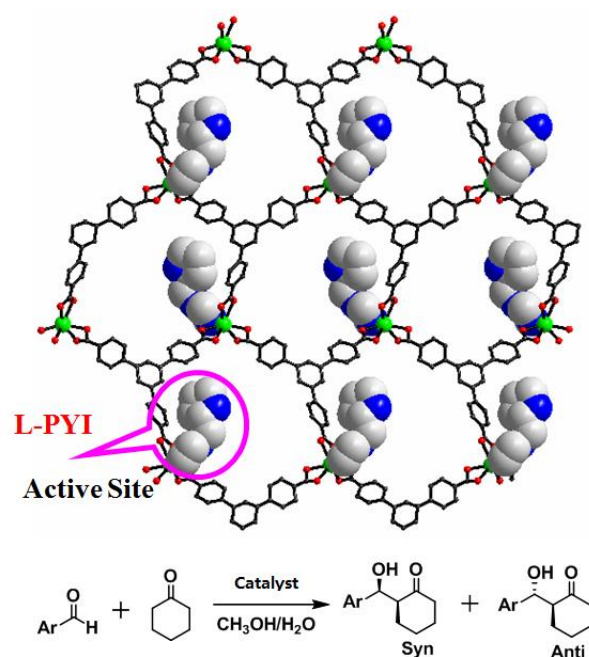
Fig. 19 The 2D honeycomb network of Cd-BTB with active L-PYI sites (space-filling model) in the pores, and the catalytic aldol reaction of aldehydes with cyclohexanone.

The photoactive MOF Zn-BCIP1 is a 2D brick wall lamellar network, built from 3-connected binuclear zinc nodes and 4,4',4''-nitrilotribenzoate (H$_3$TCA) bridges (Fig. 20).[38] The dimensions of the porous channels are of 12×16 Å^2, which contain chiral L-BCIP moieties that are coordinating with zinc ions. The homochiral MOF can be simply activated to deprotect the proline unit by heating. The resulting new MOF Zn-PYI1 is efficient on photocatalytic alkylation of aldehydes coupled with diethyl 2-bromomalonate. Zn-PYI1 catalyzes the reaction of phenylpropyl aldehyde with 2-bromomalonate to generate the corresponding product in 74% yield with excellent enantioselectivity of 92%. Similar results have been achieved when the enantiomorph Zn-PYI2 was used to prompt the reaction, besides of producing the product of opposite chirality.
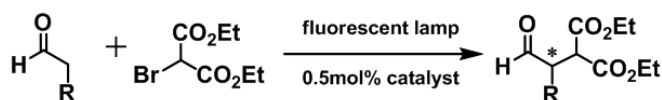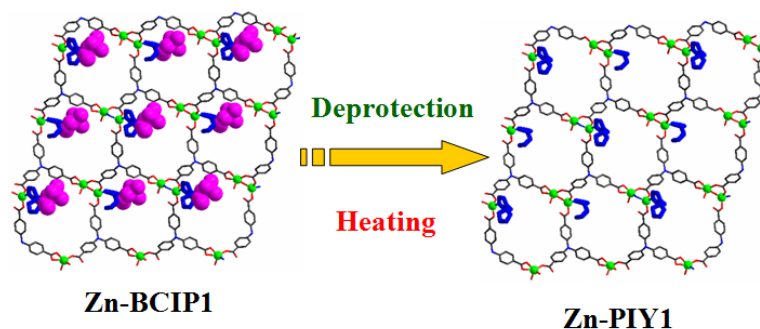
Fig. 20 Illustration of the structural transformation from Zn-BCIP1 to Zn-PYI1 by removal of the protection groups on the pyrrolidine moieties, and photocatalytic α-alkylation of aliphatic aldehydes.

7. Post-modification of metal-organic frameworks for heterogeneous catalysis

Limited by current technologies on growing high quality single crystals and single crystal X-ray diffraction structural analysis, it is not a reality to immobilize any desired functional groups onto porous MOFs in situ synthesis. Fortunately, we can graft some reactive moieties on organic linkers at the first step. These moieties, exposed on the pore surfaces of MOFs, can be further reacted with some specific moieties to generate metal-organic framework catalysts by post-synthesis.

The Lin group has designed a chiral ligand based on BINOL moiety, ((R)-6,6'-dichloro-2,2'-dihydroxy-1,1'-binaphthyl-4,4'-bipyridine, L^{14}), which was used to construct a homochiral porous MOF $[Cd_3Cl_6(L^{14})_3]$ guest (**14**).[39] In the crystal structure of **14**, the polymeric 1D zigzag $[CdCl_2]_n$ chain SBUs, formed from chloride doubly bridging Cd(II) ions, are linked by L^{14} to form a non-interpenetrated 3D network with large 1D chiral open channels of ~1.6×1.8 nm^2 in dimensions (Fig. 21). Homochiral MOF **14** was readily post-modified by taking advantage of the chiral dihydroxy groups that are accessible to $Ti(O^iPr)_4$ transferred through the large open channels. The resulted solid (designated as **15**) is highly active on the heterogeneous asymmetric catalysis of addition of diethylzinc to aromatic aldehydes with high conversions and *ee* values, which rival to those of the homogeneous analog under the

identical conditions. Control experiments with a series of dendritic aldehydes of different sizes (from 0.8 to 2.0 nm) demonstrate that catalyst **15** has interesting size-selective property, because the catalysis chiefly occurs inside the opening channels.
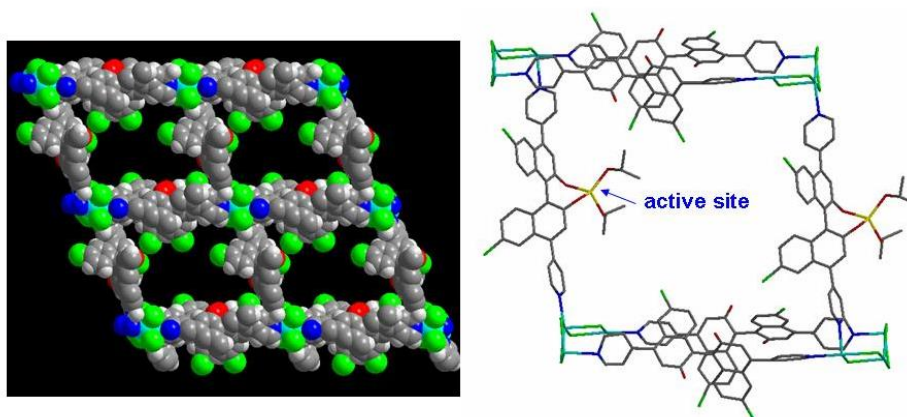
Fig. 21 (Left) Crystal structure of **14** in space-filling model, showing the large 1D chiral open channels and (Right) a schematic representation of the active (BINOLate)Ti(O^{i}Pr)$_2$ catalytic sites in the open channels of **15**.

N-heterocyclic carbenes (NHCs) and their metalated complexes are highly efficient catalysts in numerous reactions.[40] Incorporation of metal-NHCs onto the pore surfaces of porous MOFs should generate highly efficient heterogeneous catalysts. The two MOFs [Cu$_2$L^{16}$_2$(MeOH)$_2$]·guest (**16**; H$_2$L^{16} = 1,1'-methylenebis(3-(4-carboxyphenyl)-1*H*-imidazol-3-ium)) and [CuL^{16}Cl$_2$]·guest (**17**) are built from the same bifunctional aromatic azolium derivative L^{16} and Cu^{II} nodes (Fig. 22).[41] In the crystal structure of **16**, two copper ions are coupled by four carboxylate groups to form a paddle-wheel SBU, and further connected with L^{16} to form a wave-like lamellar network, containing 80-membered macrocycles (the cross dimensions of 18.05 × 34.4 Å^2). In the crystal structure of **17**, the Cu^{II} centers are linked by L^{16} to extend into a 1D zigzag chain. The NHC precursors in **16** are able to pocket palladium sites by unmasking the imidazolium moieties under mild conditions. The post-modified solid (designated as **18**) from **16** presents excellent heterogeneous catalytic activity in the Suzuki-Miyaura coupling reaction of penylhalides with

phenylboronic acids. The catalytic activity of **18** is much superior to Me$_2$L^{16} and H$_2$L^{16} supported Pd catalysts, Pd(OAc)$_2$ and Pd/C (8~37% yields). However, the post-metalated solid (designated as **19**) from **17** catalyzes the coupling reaction less efficiently under the identical conditions (43% yield). The low catalytic efficiency of **19** should be a consequence of the imidazolium groups of L^{16} that are held very close to the {CuO$_2$Cl$_2$} units linked by strong hydrogen bondings to obstruct the post-metallation and subsequent catalysis.
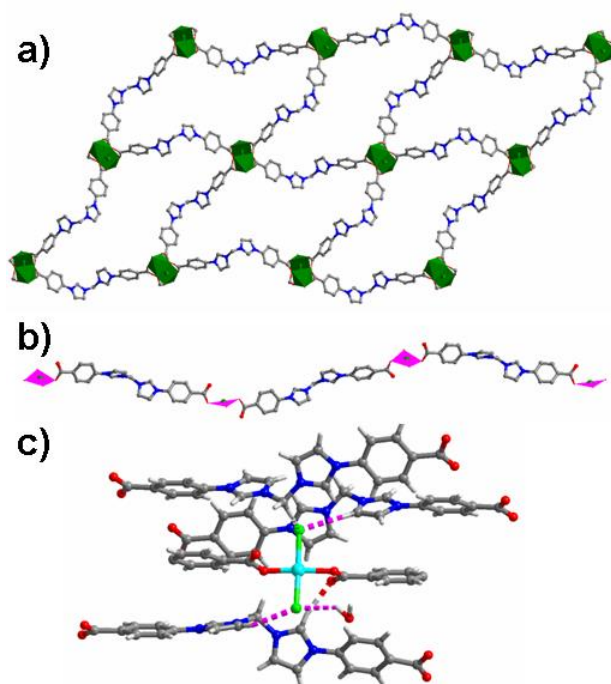
Fig. 22 (a) A view of the lamellar network of **16** consisting of 80-membered macrocycles with post-modifiable imidazolium moieties. (b) The linear network of **17**. (c) A close view of the steric congestion environments around the azolium moieties in **17**.

The metal-organic nanotube (MONT) [ZnL^{20}Cl$_2$] guest (**20**; H$_2$L^{20} = 1,1'-methylenebis(3-(4-carboxy-2-methylphenyl)-1*H*-imidazol-3-ium)) is built from L^{20} linking up tetra-coordinated zinc ions (Fig. 23).[42] MONT **20** has large 1D nanotubular channels with exterior wall diameter of 4.9 nm and interior channel diameter of 3.3 nm. Interlocking of the nanotubes gives rise to a 3D chiral framework containing 1D helical cylindered channels with diameter of 2.0 nm. The palladium metalated solid (designated as **21**) from **20** was conducted as a highly active

heterogeneous catalyst for a number of reactions. Solid **21** catalyzes the coupling reaction of a range of penylhalides with phenylboronic acids in toluene at 70 ^{o}C for 5 h, leading to almost quantitative product yields (Scheme 1). The catalytic property of **21** is superior to that of Me_2L^{20} supported Pd catalyst, $Pd(OAc)_2$ and Pd/C (1.1~42% yields) on the Suzuki-Miyaura coupling reaction under the identical conditions. Moreover, solid **21** is also highly active on the Heck coupling reaction of various aryl halides and olefins for 1 h with almost quantitative product yields (Scheme 2). The high efficiency and versatility of catalyst **21** were further demonstrated on the catalytic hydrogenation of olefins. Reactions proceed smoothly at room temperature with 0.5 mol% of **21** under 1 atm H_2 atmosphere, in which quantitative yields were achieved for a wide range of substrates after 1 h. The results cannot be reached by its constituents, such as Me_2L^{20} supported Pd catalyst, $Pd(OAc)_2$ and Pd/C (<1~5.3% yields). Moreover, solid **21** can effectively promote the reduction of large scale of (E)-ethyl cinnamate (17.6 g, 100 mmol) with 0.005 mol% catalyst loading, and the turnover number is up to 13746 after 12 h. Further more, with 0.5 mol% of **21**, nitrobenzene was fully reduced by H_2 under atmosphere pressure for 1 h at room temperature, leading to a quantitative yield of aniline.
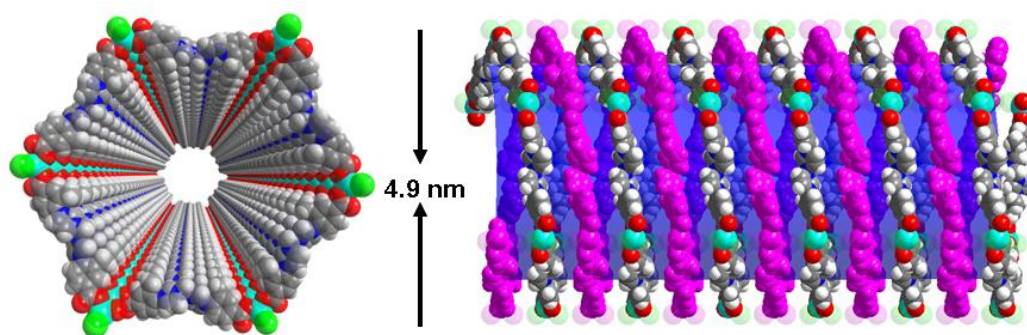
Fig. 23 Perspective (left) and side (right) views of the open-ended hollow chiral nanotube **20**.
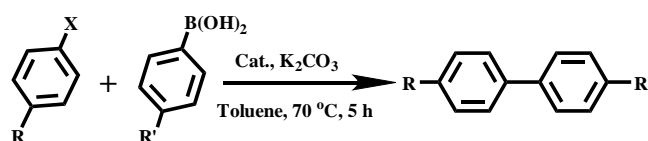
Scheme 1 Suzuki-Miyaura coupling reaction of phenylhalides and phenylboronic acids with 0.5 mol% catalyst **21**.
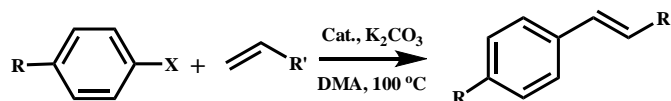
Scheme 2 Heck coupling reaction of aryl halides and olefins with 0.5 mol% catalyst **21**.

8. Conclusions and outlook

This short review highlights the approaches on rational assembly of metal-organic frameworks for heterogeneous catalysis. Even though the traditional synthesis methods have the opportunity to construct some metal-organic frameworks that contain metal sites coordinating to the volatile solvent molecules; however, because the catalytic-active metal sites are also the pivot components of MOFs, the dissociation of the coordinating solvent molecules is inevitably to destroy the porous structures in some cases. Moreover, most structural arrangements of the building synthons in MOFs are not desirable for the application in heterogeneous catalysis, because connecting the metal sites to the organic linkers often blocks metal active sites. Therefore, the use of molecular building blocks for the synthesis of metal-organic framework catalysts has been developed by fixing the catalytic-active sites on organic ligands. The facile tunability of the molecular modules allows us to precisely engineer a multitude of MOF catalysts. It is evident from the examples illustrated in this short review that the catalytic functionalities of MOFs can be designed and modulated rationally. Because their topologies are controlled by the connection between the metal coordination sites and the orientation and number of coordinating donors on the multifunctional linkers, precise selection of the structural SBUs and control of their connection ways allow us systematic modification of the pore structures. These porous materials let the active sites freely accessible to reagent molecules transferred through the opening channels. Considering that numerous homogeneous catalytic-active moieties have been readily available for the synthesis of functional linkers, we foresee that it may be a burgeoning field of the porous metal-organic framework catalysts, which should have a brilliant future and are ongoing in an explosive growth.

References

1. a) J. R. Long and O. M. Yaghi Ed., *Chem. Soc. Rev.*, 2009, **38**, 1213; b) H.-C. Zhou, J. R. Long and O. M. Yaghi Ed., *Chem. Rev.*, 2012, **112**, 673; c) H.-C. Zhou and S. Kitagawa Ed., *Chem. Soc. Rev.*, 2014, **43**, 5415.

2. a) J.-R. Li, R. J. Kuppler and H.-C. Zhou, *Chem. Soc. Rev.*, 2009, **38**, 1477; b) M. P. Suh, H. J. Park, T. K. Prasad and D.-W. Lim, *Chem. Rev.*, 2012, **112**, 782.

3. a) K. Sumida, D. L. Rogow, J. A. Mason, T. M. McDonald, E. D. Bloch, Z. R. Herm, T.-H. Bae and J. R. Long, *Chem. Rev.*, 2012, **112**, 724; b) J.-R. Li, J. Sculley and H.-C. Zhou, *Chem. Rev.*, 2012, **112**, 869; c) H. Wu, Q. Gong, D. H. Olson and J. Li, *Chem. Rev.*, 2012, **112**, 836.

4. E. Coronado and G. Minguez Espallargas, *Chem. Soc. Rev.*, 2013, **42**, 1525.

5. P. Horcajada, R. Gref, T. Baati, P. K. Allan, G. Maurin, P. Couvreur, G. Férey, R. E. Morris and C. Serre, *Chem. Rev.*, 2012, **112**, 1232.

6. Z. Hu, B. J. Deibert and J. Li, *Chem. Soc. Rev.*, 2014, **43**, 5815.

7. a) Y. Takashima, V. M. Martínez, S. Furukawa, M. Kondo, S. Shimomura, H. Uehara, M. Nakahama, K. Sugimoto and S. Kitagawa, *Nat. Commun.*, 2011, **2**, 168; b) M.-J. Dong, M. Zhao, S. Ou, C. Zou and C.-D. Wu, *Angew. Chem., Int. Ed.*, 2014, **53**, 1575; c) Q.-L. Zhu and Q. Xu, *Chem. Soc. Rev.*, 2014, **43**, 5468.

8. a) Y. Cui, Y. Yue, G. Qian and B. Chen, *Chem. Rev.*, 2012, **112**, 1126; b) B. Chen, S. Xiang and G. Qian, *Acc. Chem. Res.*, 2010, **43**, 1115; c) L. E. Kreno, K. Leong, O. K. Farha, M. Allendorf, R. P. Van Duyne and J. T. Hupp, *Chem. Rev.*, 2012, **112**, 1105.

9. a) L. Ma, C. Abney and W. Lin, *Chem. Soc. Rev.*, 2009, **38**, 1248; b) J. Lee, O. K. Farha, J. Roberts, K. A. Scheidt, S. T. Nguyen and J. T. Hupp, *Chem. Soc. Rev.*, 2009, **38**, 1450; c) A. Corma, H. García and F. X. Llabrés i Xamena, *Chem. Rev.*,

2010, **110**, 4606; d) Y. Liu, W. M. Xuan and Y. Cui, *Adv. Mater.*, 2010, **22**, 4112; e) M. Yoon, R. Srirambalaji and K. Kim, *Chem. Rev.*, 2012, **112**, 1196; f) H. R. Moon, D.-W. Lim and M. P. Suh, *Chem. Soc. Rev.*, 2013, **42**, 1807; g) J. Liu, L. Chen, H. Cui, J. Zhang, L. Zhang and C.-Y. Su, *Chem. Soc. Rev.*, 2014, **43**, 6011; h) T. Zhang and W. Lin, *Chem. Soc. Rev.*, 2014, **43**, 5982.

10. D. W. Breck, *Zeolite molecular sieves, structure, chemistry, and use*, John Wiley & Sons, New York, 1974.

11. S. S. Y. Chui, S. M. F. Lo, J. P. H. Charmant, A. G. Orpen and I. D. Williams, *Science*, 1999, **283**, 1148.

12. K. Schlichte, T. Kratzke and S. Kaskel, *Microporous Mesoporous Mater.*, 2004, **73**, 81.

13. S. M. Cohen, *Chem. Rev.*, 2011, **112**, 970.

14. G.-Q. Kong and C.-D. Wu, *Inorg. Chem. Commun.*, 2009, **12**, 731.

15. C.-D. Wu, L. Li and L.-X. Shi, *Dalton Trans.*, 2009, 6790.

16. L.-X. Shi and C.-D. Wu, *Chem. Commun.*, 2011, **47**, 2928.

17. M.-H. Xie, X.-L. Yang and C.-D. Wu, *Chem. Eur. J.*, 2011, **17**, 11424.

18. P. G. Cozzi, *Chem. Soc. Rev.*, 2004, **33**, 410.

19. S.-H. Cho, B. Ma, S. T. Nguyen, J. T. Hupp and T. E. Albrecht-Schmitt, *Chem. Commun.*, 2006, 2563.

20. F. Song, C. Wang, J. M. Falkowski, L. Ma and W. Lin, *J. Am. Chem. Soc.*, 2010, **132**, 15390.

21. J. M. Falkowski, C. Wang, S. Liu and W. Lin, *Angew. Chem., Int. Ed.*, 2011, **50**, 8674.

22. C. Zhu, G. Yuan, X. Chen, Z. Yang and Y. Cui, *J. Am. Chem. Soc.*, 2012, **134**, 8058.

23. J. Jiang, K. Kasuga and D. P. Arnold, in Supramolecular Photosensitive and Electroactive Materials, H. S. Nalwa, eds. *San Diego: Academic Press*, 2001, 113.

24. a) C. Zou and C.-D. Wu, *Dalton Trans.*, 2012, **41**, 3879; b) M. Zhao, S. Ou and C.-D. Wu, *Acc. Chem. Res.*, 2014, **47**, 1199; c) W.-Y. Gao, M. Chrzanowski and S. Ma, *Chem. Soc. Rev.*, 2014, **43**, 5841.

25. C. Zou, T. Zhang, M.-H. Xie, L. Yan, G.-Q. Kong, X.-L. Yang, A. Ma and C.-D. Wu, *Inorg. Chem.*, 2013, **52**, 3620.

26. M.-H. Xie, X.-L. Yang and C.-D. Wu, *Chem. Commun.*, 2011, **47**, 5521.

27. X.-L. Yang, M.-H. Xie, C. Zou, Y. He, B. Chen, M. O'Keeffe and C.-D. Wu, *J. Am. Chem. Soc.*, 2012, **134**, 10638.

28. X.-L. Yang, C. Zou, Y. He, M. Zhao, B. Chen, S. Xiang, M. O'Keeffe and C.-D. Wu, *Chem Eur. J.*, 2014, **20**, 1447.

29. X.-L. Yang and C.-D. Wu, *Inorg. Chem.*, 2014, **53**, 4797.

30. M.-H. Xie, X.-L. Yang, Y. He, J. Zhang, B. Chen and C.-D. Wu, *Chem Eur. J.*, 2013, **19**, 14316.

31. C. Zou, Z. Zhang, X. Xu, Q. Gong, J. Li and C.-D. Wu, *J. Am. Chem. Soc.*, 2012, **134**, 87.

32. M.-H. Xie, X.-L. Yang, C. Zou and C.-D. Wu, *Inorg. Chem.*, 2011, **50**, 5318.

33. M. H. Alkordi, Y. Liu, R. W. Larsen, J. F. Eubank and M. Eddaoudi, *J. Am. Chem. Soc.*, 2008, **130**, 12639.

34. X.-L. Yang and C.-D. Wu, *CrystEngComm*, 2014, **16**, 4907.

35. a) X.-L. Yang, M.-H. Xie, C. Zou, F.-F. Sun and C.-D. Wu, *CrystEngComm*, 2011, **13**, 1570; b) X.-L. Yang, M.-H. Xie, C. Zou and C.-D. Wu, *CrystEngComm*, 2011, **13**, 6422.

36. M. Wang, M.-H. Xie, C.-D. Wu and Y.-G. Wang, *Chem. Commun.*, 2009, 2396.

37. D. Dang, P. Wu, C. He, Z. Xie and C. Duan, *J. Am. Chem. Soc.*, 2010, **132**, 14321.

38. P. Wu, C. He, J. Wang, X. Peng, X. Li, Y. An and C. Duan, *J. Am. Chem. Soc.*, 2012, **134**, 14991.

39. C.-D. Wu, A. Hu, L. Zhang and W. Lin, *J. Am. Chem. Soc.*, 2005, **127**, 8940.

40. a) V. Nair, R. S. Menon, A. T. Biju, C. R. Sinu, R. R. Paul, A. Jose and V. Sreekumar, *Chem. Soc. Rev.*, 2011, **40**, 5336; b) G. C. Fortman and S. P. Nolan, *Chem. Soc. Rev.*, 2011, **40**, 5151.

41. G.-Q. Kong, X. Xu, C. Zou and C.-D. Wu, *Chem. Commun.*, 2011, **47**, 11005.

42. G.-Q. Kong, S. Ou, C. Zou and C.-D. Wu, *J. Am. Chem. Soc.*, 2012, **134**, 19851.

Graphical Abstract:

The recently developed strategies on designed synthesis of porous metal-organic framework catalysts and their interesting catalytic properties are summarized in this short review.

= **Active Site or Post-Modifiable Moiety**